

Hyperfine-field distribution in $\text{Fe}_3\text{Si}_{1-x}\text{Al}_x$ alloys and a theoretical interpretation

T. J. Burch

Department of Physics, Marquette University, Milwaukee, Wisconsin 53233

K. Raj

Ferrofluidics Corporation, Burlington, Massachusetts 01803

P. Jena*

Materials Science Division, Argonne National Laboratory, Argonne, Illinois 60439

J. I. Budnick

Department of Physics and Institute of Materials Science, University of Connecticut, Storrs, Connecticut 06268

V. Niculescu

Virginia Commonwealth University, Richmond, Virginia 23284

W. B. Muir

Department of Physics, McGill University, Montreal, Quebec, H3A 2K6 Canada

(Received 7 August 1978)

In $\text{Fe}_3\text{Si}_{1-x}\text{Al}_x$ alloys with small x the Si and Al nuclear magnetic resonances are 31.5 and 16.1 MHz, respectively. The concentration dependences of the frequencies of these resonances are linear, the Si resonance shifting to lower frequencies, the Al resonance to higher frequencies. Both the magnitudes and concentration dependences of the Si and Al internal fields are in agreement with the predictions of a simple model which Jena and Geldart, following the approach of Daniel and Friedel, have found successful in calculating the fields of sp elements in Heusler alloys. A positive sign is predicted for the Si internal field, and a negative sign for the Al field. Magnetization and lattice-parameter data required for the comparison of experiment and theory are also reported.

I. INTRODUCTION

In this paper we present experimental results for the hyperfine fields in the alloy system $\text{Fe}_3\text{Si}_{1-x}\text{Al}_x$ over the entire range of Al substitutions, extending previously published results for $x < 0.25$.¹ We find a systematic concentration dependence of the internal fields of the sp elements Al and Si. Finally we show that the measured magnitudes and the signs of these fields are in reasonable agreement with those predicted by the model of Jena and Geldart, a model which has been successful in calculating the magnitudes and signs of the internal fields of sp elements in both Fe, Co, and Ni hosts and in Heusler alloys.²

Fe_3Si has the D0_3 crystal structure but can be viewed as a Heusler-like alloy with the $L2_1$ structure and the formula $\text{Fe}(A,C)_2\text{Fe}(B)\text{Si}$.³ Both the A , C and B sites, the transition metal sites, are occupied by Fe; while the D sites, the sp sites, are filled by Si. See Fig. 1 for a more complete description of these sites. In Fe_3Si both the B and the A, C sites carry moments which not only differ in magnitude ($2.2\mu_B$ and $1.35\mu_B$, respectively), but also react independently to transition-metal impurity substitutions.⁴ In this paper, the effect of sp impurities on the sublattice moments is investigated and the model of Jena and Geldart is

applied for the first time to a system with two independent sublattice magnetizations.

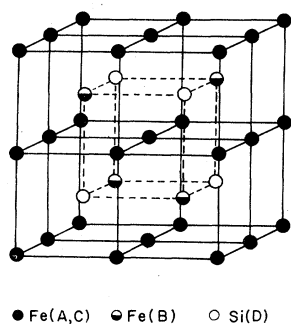
II. PREVIOUS EXPERIMENTAL RESULTS ON Fe_3Si AND Fe_3Al

A continuous range of similar bcc solid solutions form in the $\text{Fe}_3\text{Si}_{1-x}\text{Al}_x$ alloy system over the entire range of x . The end points of this range Fe_3Si and Fe_3Al have been extensively studied. A summary of some relevant crystallographic and magnetic properties is given in Table I. Comparison of these two alloys shows that though essentially similar, significant differences exist.

The lattice parameter, 0.104 \AA larger in Fe_3Al than in Fe_3Si , is a linear function of x for the entire series of alloys with $a = 5.653 + 0.140x$.

The local moments and internal fields are quite comparable in the two compounds. On the $\text{Fe}(B)$ sites the values are $2.2\mu_B$ and -335 kOe , respectively, suggesting that this site is similar to Fe in Fe metal. Both the moments and internal fields of Fe on the A, C sites are somewhat larger in Fe_3Al ($1.45\mu_B$ and -234 kOe) than in Fe_3Si ($1.35\mu_B$ and -218 kOe). The Al and Si atoms carry essentially 0 moment and have internal fields of 26 and 37 kOe, respectively. The sign of the Si field is positive,¹⁶ while that of the Al field is unknown.

The alloys used in this work were prepared by



SITE	1nn	2nn	3nn	4nn	5nn
Fe(A,C)	4 Fe(B) 4 Si	6 Fe(A,C)	12 Fe(A,C)	12 Fe(B) 12 Si	8 Fe(A,C)
Fe(B)	8 Fe(A,C)	6 Si	12 Fe(B)	24 Fe(A,C)	8 Si
Si	8 Fe(A,C)	6 Fe(B)	12 Si	24 Fe(A,C)	8 Fe(B)

FIG. 1. Unit cell of the $L2_1$ crystal structure. The B and A,C sites are occupied by Fe. The D sites by Si and/or Al. The inset shows the nearest neighbors for each of these sites.

methods described elsewhere.^{1,3} In short, alloys with $0 \leq x \leq 0.12$ were heat treated like Fe_3Si , and those with $0.12 \leq x \leq 1.0$ like Fe_3Al . All of the samples were analyzed by x-ray diffraction. Some samples with large x had very small amounts of a second phase. Since the spin-echo spectrum for alloys with large x is completely dominated by a broad Al spectrum, the presence of such a second phase will not materially affect the NMR results. The lattice parameters shown in Fig. 2 were obtained from this x-ray data.

The magnetization of all samples was measured at room temperature with a vibrating sample magnetometer. These data show some scatter (thought to arise from varying amounts of crystallographic disorder in the alloys and, in some cases, also from the presence of the second phase), but in gen-

eral the magnetization increases linearly with x .

Spin-echo spectra (plots of normalized echo amplitude versus frequency) at 1.3 K are shown in Fig. 3 for some representative $\text{Fe}_3\text{Si}_{1-x}\text{Al}_x$ alloys. Resonance due to Fe(B), Fe(A,C), Si(D), and Al(D) nuclei occur in these spectra. In the $x=0$ sample, Fe_3Si , the resonances due to Fe(B), Fe(A,C), and Si(D) nuclei are at 46.6, 30.0, and 31.5 MHz, respectively. All of the lines are very narrow in frequency because of the homogeneous environments characteristic of alloys with a high degree of long-range atomic order.

In the spectra of alloys with small additions of Al ($0 \leq x \leq 0.25$) an additional line is seen at about 16.1 MHz. This line is due to Al nuclei on the D sites. Comparison of these spectra shows that all of the lines get progressively broader and develop satellites of increasing intensity as x increases. The relative intensities of the main lines and corresponding satellites are approximately the probabilities of the different near-neighbor environments produced by a random substitution of Al for Si on the D sites.

For small increases of x the Al(D) resonance shifts to higher frequency while the Si(D), Fe(B), and Fe(A,C) resonances shift to lower frequency. See Figs. 4 and 5.

For larger values of x ($0.25 < x \leq 1.0$) the intense Al resonance mixes with the weaker Fe(A,C) and Si(D) resonances making them impossible to separate. The linear concentration dependence of the Al(D) internal field holds in this region. Since the Si resonance cannot be isolated from the Al and Fe(A,C) signals the internal fields of Si(D) have not been determined for the region $0.25 \leq x \leq 1.0$. The resonant frequencies of Fe(B) in this region are almost constant with x while that of Fe(A,C) must go through a shallow minimum and then increase to its value in Fe_3Al . The Fe fields in Fe_3Al are known through Mössbauer experiments.¹⁰

TABLE I. Listing of crystallographic and magnetic properties of Fe_3Si and Fe_3Al for purposes of comparison.

	Fe_3Si	Fe_3Al
Crystal structure	DO_3 (Heusler, Ref. 6)	DO_3 (Heusler, Ref. 6)
Lattice constant	5.653 Å (Ref. 6)	5.793 Å (Ref. 6)
Magnetic structure	Ferro (Ref. 5)	Ferro (Ref. 5)
Curie temperature	840 K (Ref. 5)	713 K (Ref. 5)
Moments	Fe(B) = $2.2\mu_B$ (Refs. 4, 12, 13) Fe(A,C) = $1.35\mu_B$ Si $\sim 0\mu_B$	Fe(B) = $2.2\mu_B$ (Ref. 14) Fe(A,C) = $1.45\mu_B$ Al $\sim 0\mu_B$
Internal fields	Fe(B) = 338 kOe (Refs. 7, 11) Fe(A,C) = 218 kOe Si(D) = 37 kOe	Fe(B) = 330 kOe (Refs. 8, 10) Fe(A,C) = 234 kOe Al(D) = 26 kOe

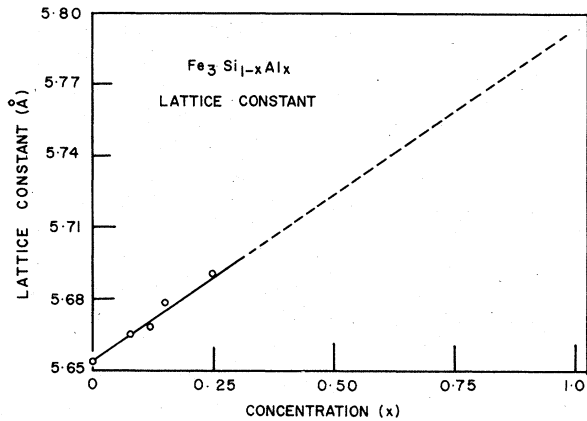


FIG. 2. Concentration dependence of the lattice parameter of the $Fe_3Si_{1-x}Al_x$ alloys. The data are from this work.

See Fig. 5. The values of the Fe internal fields in Fe_3Si and Fe_3Al are consistent with the values of their Fe moments. The Fe(B) moment is $2.2\mu_B$ in both alloys. The Fe(A,C) moment is $0.1\mu_B$ larger in Fe_3Al than in Fe_3Si . Since the internal

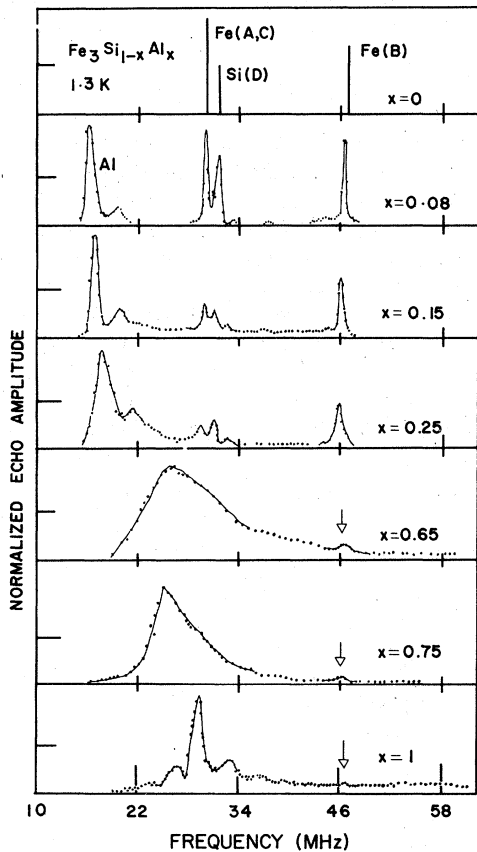


FIG. 3. Spin-echo spectra, plots of normalized echo amplitude vs frequency, of $Fe_3Si_{1-x}Al_x$ alloys for the concentrations indicated.

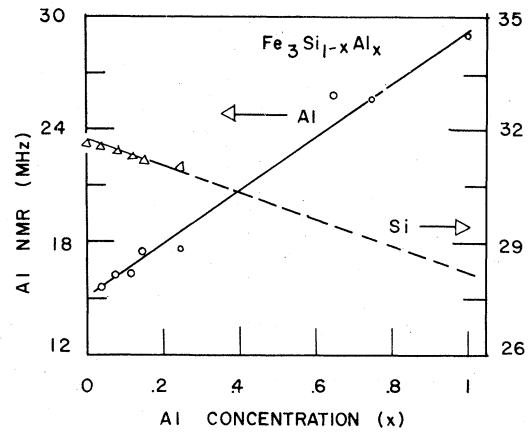


FIG. 4. Concentration dependences of the resonant frequencies of Al(D) and Si(D) nuclei in $Fe_3Si_{1-x}Al_x$ alloys.

fields of Fe atoms in these alloys are very nearly proportional to their atomic moments, with $1\mu_B$ equivalent to about 21 MHz or 150 kOe the near equality of the Fe(B) fields and 2-MHz shift in the Fe(A,C) fields seems explained. We are unable to say, at the present time, whether the small changes in internal fields between Fe_3Si and Fe_3Al are due to small changes in the local Fe moments or to some other mechanism, perhaps connected with the reduction of the number of conduction electrons by Al substitution.⁹

The change in the magnitude of the Al fields seems linear with concentration with $\nu_{Al} = 16.1 + 13x$. It should be noted that because of the broad asymmetrical distributions for large x the Al fields are plotted as the center of gravity of a spectrum rather than a peak value. The Si fields are given by $\nu_{Si} = 31.5 - 3.5x$ at low Al concentrations and an extrapolation to higher concentrations is made. It will be shown later that this behavior

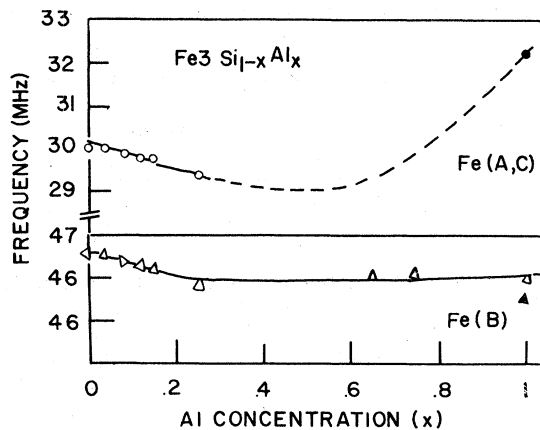


FIG. 5. Concentration dependence of the resonant frequencies of Fe(A,C) and Fe(B) nuclei in $Fe_3Si_{1-x}Al_x$ alloys.

can be explained if the sign of the Al internal field is assumed to be negative, opposite that of Si, and if the negative contribution due to conduction electrons increases as conduction electrons are removed from the system by replacing Si with Al.

III. CALCULATION OF SI AND AL INTERNAL

Jena and Geldart, following the approach of Daniel and Friedel have proposed a model for calculating the hyperfine fields of the sp elements in Heusler alloys and the ferromagnetic hosts Fe, Ni, and Co.² In this model the spin density used to calculate a hyperfine field is found by solving Schrödinger's equations with a square-well potential for the nonmagnetic ions. The model's application to $\text{Fe}_3\text{Si}_{1-x}\text{Al}_x$ alloys will be outlined and the assumptions and approximations necessary will be discussed.

The ferromagnetic host is considered to be a lattice of magnetic moments and a homogeneous electron gas, split into a majority (\uparrow) and a minority (\downarrow) spin band by the localized magnetic moments (primarily due to d electrons) at the Fe(B) and Fe(A, C) sites. Although this system contains two different magnetic moments, for the purposes of this calculation, it will be treated by assigning the average sublattice moment ($1.6\mu_B$) to each Fe site. The Fe moments split the conduction band into two subbands. A band splitting parameter Δ is determined empirically by requiring that the hyperfine field of Si in Fe_3Si calculated from the Jena-Geldart model equals the measured value. Once chosen, Δ is allowed to scale with the measured magnetic moment per Fe atom of the alloys, $\bar{\mu}(x)$. This scaling leads to a value $\Delta/E_F(x) = 0.26\bar{\mu}(x)/\mu_B$, where $E_F(x)$ is the Fermi energy, and

$$\bar{\mu}(x) = \frac{1}{12} \{4\mu_{\text{Fe}(B)}(x) + 8\mu_{\text{Fe}(A, C)}(x)\}.$$

The spin-independent Fermi wave vector of the system in the free-electron approximation is given by

$$k_F^3/3\pi^2 = n_0,$$

where n_0 is the sp electron density of the system. In calculating n_0 , Al and Si atoms are assumed to donate three and four sp electrons, respectively, to the conduction band. To estimate the contribution from the magnetic ions, it is assumed that the d electrons are localized compared to sp electrons and that there are 5 electrons in the spin-down state $Z_d\downarrow$. The value of $Z_d\uparrow$ at both Fe sites is then obtained for each alloy from the measured values of their magnetizations.

$$Z_d\uparrow - Z_d\downarrow)_{B, AC} = \mu_{\text{Fe}(B, AC)}/\mu_B.$$

The sp electron contributions to the conduction

band from the B and A, C sites are

$$[Z_{sp}]_{B, AC} = 8 - (Z_d\downarrow + Z_d\uparrow)_{B, AC}.$$

In Fe_3Si , $[Z_{sp}]_B$ and $[Z_{sp}]_{AC}$ are 0.2 and -0.65 electrons, respectively, yielding

$$n_0 = \frac{Z_{av}}{\Omega_0} = \frac{8(-0.65) + 4(0.2) + 4(4)}{a_L^3},$$

where a_L , Z_{av} , and Ω_0 are the lattice constants, the average number of electrons per unit cell and the volume per unit cell in the alloy.

The effective impurity potentials of the nonmagnetic ions Si and Al are simulated by an effective charge Z^* .

$$Z^* = Z_{\text{val}} - Z_{av},$$

where Z_{val} is 4 for Si and 3 for Al, and Z_{av} equals $n_0\Omega_0$.

The effective potentials are represented by a spin-dependent square well (approximating a pseudopotential), whose range, $a = 3.65a_0$, is that of a typical screening potential of the ion. The depth of the well for each spin is self-consistently fixed² by requiring that the Friedel sum rule¹⁵

$$Z^{o*} = \frac{1}{\pi} \sum_l (2l+1) \delta_l [k_F^o]$$

be satisfied. The Z^{o*} are the induced screening charges, and δ_l is the partial-wave phase shift. It is assumed that the screening is essentially complete within the unit cell. A square-well potential is chosen for simplicity since for this potential, the solutions to the Schrödinger equation, and therefore the electron densities per spin, are analytic. The analytical expressions are useful in analysis of the systematics of hyperfine-field data. Because of the approximate nature of the potentials, the systematic trends and the signs of the fields obtained from theory are more reliable than the calculated magnitudes of the fields.

The hyperfine field at Al or Si is computed from the formula

$$H_{\text{hf}} = -\frac{8}{3}\pi\mu_B\alpha^2(k_F)P(0),$$

where $\alpha^2(k_F)$, the core enhancement factor,² is obtained by orthogonalizing the plane wave of wave vector k_F , to the occupied atomic core orbitals of the ion under consideration. This enhancement factor, computed for various values of k_F appropriate to the compositions of the alloys, is a slowly varying function of x .

$P(0) = n\downarrow(0) - n\uparrow(0)$ is the net electron spin density. The electron density per spin $n^\sigma(0)$ is calculated by solving the Schrödinger equation with the spin-dependent square-well potential. The parameters entering this potential are the width of the square well, the depth of the square well, the

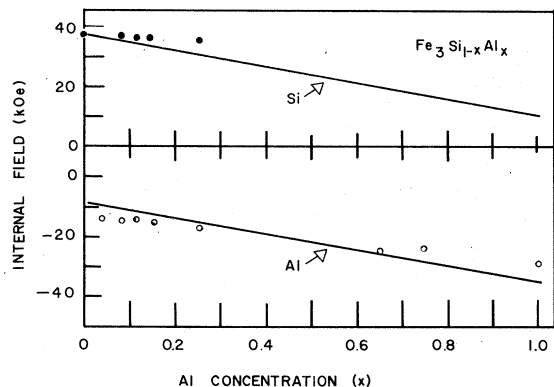


FIG. 6. Comparison of the concentration dependences of the calculated hyperfine fields (solid lines) and the experimental values for Al (open circles) and Si (dark circles).

band splitting, and the Fermi wave vector.

Since $P(0)$ is the principle variable in the expression for H_{hf} , the systematics and signs of the Al and Si fields are contained in this term. We find that the hyperfine field at a nonmagnetic site depends on a delicate cancellation between a positive contribution from electron state densities, (dependent on k_F) and a negative contribution from the spin dependence of the wave function (determined by Δ).

Therefore the concentration dependence of H_{hf} is due to the changes in k_F , the Fermi wave vector, and Δ , the band splitting parameter. The former is affected by the changing lattice constant and the average number of electrons per atom. The latter is proportional to the observed average magnetic moment per atom.

The hyperfine fields calculated for Al and Si nuclei in $\text{Fe}_3\text{Si}_{1-x}\text{Al}_x$ are shown in Fig. 6 as solid lines and can be compared with the measured Si and Al fields plotted as points.

A positive sign is calculated for the Si hyperfine field in agreement with the sign measured for Si in Fe_3Si by Kumagai *et al.*¹⁶ The sign calculated for the Al field is negative. Comparison of the measured fields with the calculated trends shows good agreement.

The negative field predicted for Al has not been confirmed by a measurement of the field dependence of its hyperfine field because of the loss of domain wall enhancement and the broadening of the resonant line, due to a distribution of demag-

netizing factors in powdered samples, when an external magnetic field is applied. The sign of this field can be inferred from the calculation because of the overall agreement between the model and the composition dependences of the data. The fact that the Al field in Fe is negative¹⁷ makes such an assignment seem reasonable.

One should be reminded that the only adjustable parameter in the theory is Δ , the band splitting, the magnitude of which was fixed for Si in Fe_3Si and then allowed to scale with the magnetization. Without any further adjustment, the fields at Si in alloys with other compositions and at Al for all values of x were calculated. Considering the approximations made, the magnitudes of the calculated Al fields agree well with the measured fields.

The magnitudes of both the observed and calculated fields of Si and Al decrease with increasing x . The calculated fields, however, decrease more rapidly. Their decrease is due principally to a reduction of the positive Pauli paramagnetic contribution due to the decrease in the electron density of the host as x increases.

In this model, the explicit contribution of $3d$ electrons on Fe(B) and Fe(A, C) sites are neglected. Due to the itinerant character of some of the d electrons, there is an overlap of the $3d$ and sp electrons on the nonmagnetic sites. The $3d$ contributions should be positive and that from the A, C sites should be more significant since Fe(A, C) atoms are the first neighbors to Al and Si. Moreover, this contribution becomes more important as $\mu_{A,C}(x)$ increases with x . Specific contributions from $3d$ electrons are difficult to include in this free-electron model.

The goal of this section is to provide a reasonable basis for the general systematics observed for both the Al and Si fields. More involved treatments of these systematics would be necessary to provide more detailed quantitative predictions. This system seems especially interesting as a subject for such calculations and for further experiments since the preservation of the DO_3 structure ensures to a rather good degree a constant ratio of sp element to Fe in the local environments about the Al and Si sites.

ACKNOWLEDGMENT

This work has been supported in part by the University of Connecticut Research Foundation and the U. S. Department of Energy.

*Present address: Physics Dept., Michigan Technological Univ., Houghton, Mich. 49931.

¹V. Niculescu, K. Raj, T. J. Burch, and J. I. Budnick, *J. Phys. F* **7**, L73 (1977).

²P. Jena and D. W. Geldart, *Solid State Commun.* **15**, 139 (1974); *J. Magnetism Magn. Mater.* **8**, 99 (1978).

³T. J. Burch, T. Litrenta, and J. I. Budnick, *Phys. Rev. Lett.* **33**, 421 (1974).

- ⁴W. A. Hines, A. H. Menotti, J. I. Budnick, T. J. Burch, T. Litrenta, V. Niculescu, and K. Raj, *Phys. Rev. B* **13**, 4060-4068 (1976).
- ⁵M. Hansen, *Constitution of Binary Alloys* (McGraw Hill, New York, 1958).
- ⁶W. B. Pearson, *Handbook of Lattice Spacings and Structure of Metals* (Pergamon, Oxford, 1958).
- ⁷J. I. Budnick, S. Skalski, T. J. Burch, and J. H. Wernick, *J. Appl. Phys.* **38**, 1137 (1967).
- ⁸T. J. Burch, J. J. Murphy, J. I. Budnick, and S. Skalski, *J. Appl. Phys.* **41**, 1327 (1970).
- ⁹J. B. Goodenough, *Phys. Rev.* **120**, 67 (1960).
- ¹⁰M. B. Stearns, *J. Appl. Phys.* **35**, 1095 (1964).
- ¹¹M. B. Stearns, *Phys. Rev.* **129**, 1136 (1963).
- ¹²A. Paoletti and L. Passari, *Nuovo Cimento* **32**, 25 (1964).
- ¹³D. Meinhardt and O. Krisement, *Z. Phys.* **174**, 472 (1963).
- ¹⁴S. J. Pickart and R. Nathans, *Phys. Rev.* **123**, 1163 (1961); R. Nathans, M. T. Pigott, and C. G. Shull, *J. Phys. Chem. Solids* **6**, 38 (1958).
- ¹⁵E. Daniel and J. Friedel, *J. Phys. Chem. Solids* **24**, 1601 (1963).
- ¹⁶K. Kumagai, K. Asayama, and I. A. Campbell, *J. Phys. Soc. Jpn.* **37**, 1460 (1974).
- ¹⁷M. Kontani and J. Itoh, *J. Phys. Soc. Jpn.* **22**, 354 (1967).